Optoacoustic technique for noninvasive monitoring of blood oxygenation: a feasibility study

Rinat O. Esenaliev, Irina V. Larina, Kirill V. Larin, Donald J. Deyo, Massoud Motamedi, and Donald S. Prough

Replacement of invasive monitoring of cerebral venous oxygenation with noninvasive techniques offers great promise in the management of life-threatening neurologic illnesses including traumatic brain injury. We developed and built an optoacoustic system to noninvasively monitor cerebral venous oxygenation; the system includes a nanosecond Nd:YAG laser and a specially designed optoacoustic probe. We tested the system *in vitro* in sheep blood with experimentally varied oxygenation. Our results demonstrated that (1) the amplitude and temporal profile of the optoacoustic waves increase with blood oxygenation in the range from 24% to 92%, (2) optoacoustic signals can be detected despite optical and acoustic attenuation by thick bone, and (3) the system is capable of real-time and continuous measurements. These results suggest that the optoacoustic technique is technically feasible for continuous, noninvasive monitoring of cerebral venous oxygenation.

OCIS codes: 040.1880, 110.7050, 120.4290, 170.1460, 170.4580.

1. Introduction

Continuous, noninvasive monitoring of blood oxygenation (oxyhemoglobin saturation) in the brain, heart, liver, and other organs is currently not clinically feasible but would be invaluable for the management of many life-threatening illnesses, including severe traumatic brain injury, ischemia, sepsis, and shock. In critically ill neurologic patients, particularly those with traumatic brain injury, invasive monitoring of cerebral blood oxygenation and brain tissue oxygenation is now routinely performed in tertiary care centers, and information obtained from such monitors is routinely used to direct therapy.[1,2] Noninvasive monitoring of cerebral blood oxygenation would be a major advance in neurologic critical care because it would permit broader application of physiologically based therapy and would also permit earlier initiation of monitoring, even in prehospital emergency vehicles. Despite years of effort, however, there presently is no system for accurate, noninvasive, and continuous monitoring of cerebral blood oxygenation.

To date, most attempts to engineer noninvasive monitors of brain oxygenation have used near-infrared (IR) spectroscopy, which remains a promising method[3,4] that utilizes well-established differences in optical absorption coefficients of oxyhemoglobin and deoxyhemoglobin.[5,6] However, this technique has limitations associated with strong light scattering and attenuation in tissues[7] that result in limited accuracy and depth of monitoring. At present, near-IR spectroscopy cannot provide reliable and quantitative measurement of cerebral blood oxygenation, at least in part because it assesses hemoglobin saturation in a heterogeneous area of brain tissue and cannot distinguish venous from arterial blood. The development of near-IR monitoring of blood oxygenation also has been slowed by the difficulty posed by measurement or estimation of the path length of scattered light through tissues.[8] As a consequence, the technique has yet to be incorporated into routine clinical practice. However, the technology continues to improve as investigators develop more accurate methods of quantifying the signal.[9,10]

We proposed to develop an optoacoustic technique that would utilize the differences in optical absorption coefficients of oxyhemoglobin and deoxyhemoglobin to accurately monitor and quantify blood oxygenation.[11]

The authors are with the University of Texas Medical Branch, 301 University Boulevard, Galveston, Texas 77555. R. O. Esenaliev (rinat.esenaliev@utmb.edu), I. V. Larina, and K. V. Larin are with the Laboratory for Optical Sensing and Monitoring and the Department of Physiology and Biophysics. R. O. Esenaliev, I. V. Larina, K. V. Larin, and M. Motamedi are with the Center for Biomedical Engineering. R. O. Esenaliev, D. J. Deyo, and D. S. Prough are with the Department of Anesthesiology.

Received 1 October 2001; revised manuscript received 12 April 2002.

0003-6935/02/224722-10$15.00/0

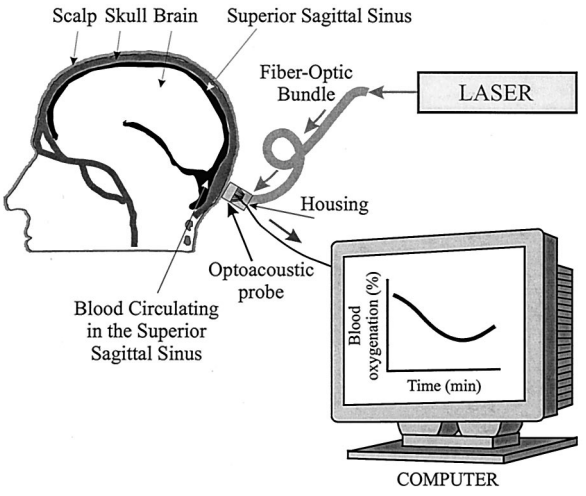

Fig. 1. Novel optoacoustic system for cerebral blood oxygenation monitoring.

In the optoacoustic technique, short laser pulses generate ultrasonic (optoacoustic) waves in absorbing media. An acoustic transducer then detects these waves, and time resolution of the resulting signal determines the depth from which the signal was derived.[12] Because scattering and attenuation of ultrasonic waves in tissues are much less compared with those of light waves, detection and analysis of the temporal characteristics and amplitude of the optoacoustic pressure waves can be used for tissue characterization with submillimeter resolution.[13–17] The high resolution of the optoacoustic technique may yield accurate measurement of blood oxygenation directly from blood vessels or localized tissues.

The superior sagittal sinus (SSS), a large central cerebral vein that is located immediately beneath the top of the human skull in the midline, represents one of the potential sites for optoacoustic monitoring of cerebral blood oxygenation (Fig. 1). After traumatic brain injury and during cardiopulmonary bypass, low oxygenation of blood circulating in the cerebral venous circulation is strongly associated with poor outcome, including disability or death.[18,19] Specially designed probes may provide optimum conditions for laser irradiation of the SSS and sensitive detection of the induced optoacoustic waves.

We designed and built an optoacoustic system that incorporates (1) a nanosecond Nd:YAG laser for generation of optoacoustic waves; (2) an optoacoustic probe containing both optical fibers for laser light delivery and piezoelectric detectors of optoacoustic waves; and (3) an electronic system for signal amplification, acquisition, and recording with a PC. Using the system, we performed *in vitro* tests in sheep blood at different oxygenation and in tissue phantoms simulating conditions typical for *in vivo* monitoring of blood oxygenation in large blood vessels.

2. Theoretical Background

Absorption of light energy in a medium is followed by rapid thermal relaxation and a temperature increase in the medium. Thermal expansion of the irradiated medium induces mechanical stress (pressure rise). This mechanism is referred to as the thermo-optical mechanism of pressure generation.[12] A short optical pulse with the incident fluence F_o induces a pressure rise $P(z)$ in the medium (without optical scattering) upon the condition of stress confinement[12]:

$$P(z) = (\beta c_s^2/C_p)\mu_a F = \Gamma \mu_a F(z) = \Gamma \mu_a F_o \exp(-\mu_a z), \quad (1)$$

where β (1/°C) is the thermal expansion coefficient, c_s (cm/s) is the speed of sound, C_p (J/g °C) is the heat capacity at constant pressure, $F(z)$ (J/cm^2) is the fluence of the optical pulse, and μ_a (cm^{-1}) is the absorption coefficient of the medium. The optoacoustic pressure in Eq. (1) can be expressed in joules per cubic centimeter or in bars (1 J/cm^3 = 10 bars). The expression $(\beta c_s^2/C_p)$ in Eq. (1) represents the dimensionless Grüneisen parameter Γ. The exponential attenuation of the optical radiation in the medium is represented by $\exp(-\mu_a z)$.

The condition of stress confinement means that there is insignificant stress relaxation in the irradiated volume during the optical pulse. Nanosecond laser pulses can be used to generate conditions of stress confinement for many optoacoustic applications.

According to Eq. (1), optoacoustic pressure amplitude is proportional to the Grüneisen parameter, fluence, and absorption coefficient of the medium, whereas the pressure spatial profile is dependent on the absorption coefficient.

Because z and t are related by the simple equation

$$z = c_s t, \quad (2)$$

the spatial distribution of laser-induced pressure $P(z)$ is detected by a wide-band acoustic transducer as a temporal profile $P(t)$:

$$P(t) = \Gamma \mu_a F_o \exp(-\mu_a c_s t). \quad (3)$$

Therefore, by recording and analyzing the temporal profile of optoacoustic waves, one can measure the absolute value of the absorption coefficient of the irradiated medium.

Most tissues are strongly scattering media in the visible and near-IR spectral range. Three major optical parameters are responsible for distribution of light in tissues: the absorption (μ_a), scattering (μ_s), and effective attenuation (μ_{eff}) coefficients. The effective attenuation coefficient is related to μ_a, μ_s, and the anisotropy factor (g), thus

$$\mu_{\text{eff}} = \{3\mu_a[\mu_a + \mu_s(1 - g)]\}^{1/2}, \quad (4)$$

where $\mu_s(1 - g)$ is the reduced scattering coefficient μ_s'.[6] Light penetration depth in tissues is defined as $1/\mu_{\text{eff}}$. Absorption and reduced scattering coefficients of tissues are low in the near-IR spectral range (from 600 to 1300 nm), which results in deeper penetration of near-IR radiation compared with that of

other parts of the spectrum. Application of near-IR radiation will allow sufficient penetration of light in tissues for optoacoustic monitoring of blood oxygenation.

Hemoglobin has a high absorption coefficient in the visible and near-IR spectral range.[6] Moreover, the hemoglobin absorption coefficient is dependent on hemoglobin saturation (i.e., oxygenation). Therefore both the amplitude and the spatial distribution of the generated optoacoustic pressure induced in blood are dependent on oxygenated hemoglobin concentration.

We anticipated that high z-axial resolution of the optoacoustic technique would permit direct measurement of blood oxygenation in the SSS because the optoacoustic waves induced in the blood would arrive at the acoustic transducer at the time defined by Eq. (2).

3. Materials and Methods

We developed and built a system for optoacoustic monitoring of blood oxygenation with the following components: (1) a Q-switched nanosecond Nd:YAG laser (Quanta-Ray, DCR-11, Spectra-Physics Inc., Mt. View, Calif.), (2) a fiber-optic light delivery system combined with a sensitive acoustic transducer in an optoacoustic probe, and (3) a computer for signal registration and processing. The laser generates 10-ns pulses at the wavelength of 1064 nm (fundamental harmonic) with an energy level as great as 0.1 J and a repetition rate as high as 5.0 Hz. Laser fluence incident on the samples was 0.1 J/cm^2, and the repetition rate was 1 Hz. In some experiments, we used laser fluence below 0.1 J/cm^2.

The laser head was coupled with one end of a fiber-optic bundle. The other end of the bundle was incorporated into the optoacoustic probe. The optoacoustic probe combines a sensitive polyvinylidene fluoride piezoelement with a diameter of 8.0 mm and optical fibers with a diameter of 0.2 mm surrounding the piezoelement. Axial resolution of the optoacoustic probe as defined by the bandwidth of the piezoelement was 0.3 mm. This probe allowed measurement in the backward mode—irradiation and detection from the same side of the samples. In experiments in the forward mode (irradiation and detection from opposite sides), we used acoustic transducers without a fiber-optic light delivery system. Preamplifiers with low input capacitance then amplified the signals from the optoacoustic probe and acoustic transducers. The amplified signals were recorded by a portable digital scope (TDS 520, Tektronix Inc., Beaverton, Ore.) and stored on a computer (Dell Computer Corp., Round Rock, Tex.; the processor was a Pentium III, 550 MHz).

Arterial and venous blood samples (total hemoglobin concentration was 5.0 g/dl) were taken from sheep femoral and pulmonary arteries, respectively. The artery and vein were catheterized, and blood was taken with a 5-ml syringe filled with heparin. To obtain systemic venous blood with low oxygenation (analogous to low cerebral oxygenation during brain hypoperfusion), hemorrhagic shock was induced in the sheep. A spectrophotometric cuvette with a thickness of 1.0 cm was used in the first set of experiments [Fig. 2(a)]. To prevent the contact of blood with air, we placed a mineral oil film (thickness of 3 mm) over the bottom of the cuvette. We then injected blood (total volume of 2.0 ml) into the cuvette using a syringe with a needle that passed under the mineral oil film. Pure arterial and pure venous blood as well as their mixtures were used in the experiments. The arterial and venous blood were mixed in the cuvette in different proportions to vary the blood oxygenation. Immediately after optoacoustic data acquisition, blood was taken from the cuvette with 1.0-ml syringes, and oxygenation measurements were performed with a standard CO-Oximeter (IL 813 Instrumentation Laboratories, Lexington, Mass.).

We performed studies demonstrating the capability of the optoacoustic technique to monitor rapid changes in blood oxygenation continuously and in real time. The changes in oxygenation were induced by air insufflation into venous blood in the cuvette for several seconds. Air insufflation rapidly increased blood oxygenation. Optoacoustic signals were recorded after each insufflation.

Bovine bone slabs with thicknesses of 4.0–13.0 mm were used to simulate a human skull. In these experiments, we measured transmission of laser light [Fig. 2(b)] and optoacoustic waves [Fig. 2(c)] through bone tissue. Laser pulses were directed onto the bone slab of different thickness [Fig. 2(b)] placed on top of an absorbing phantom (absorbing aqueous solution of Naphthol Green, a dye that absorbs light at the Nd:YAG laser wavelength, in a plastic vessel). The solution had optical properties typical of normal venous blood. The amplitude of the optoacoustic signal generated in the absorbing phantom was dependent on the thickness of the bone slab. This allowed measurement of optical transmission through bone tissue. To measure acoustic transmission of optoacoustic pulses through bone, laser pulses were directed onto the same absorbing phantom placed on top of the bone slab [Fig. 2(c)]. To simulate laser irradiation of blood and detection of the induced optoacoustic signal through bone, we performed a set of experiments using two bones (with thicknesses of 4.5 and 4.8 mm) with the absorbing solution placed between them [Fig. 2(d)].

Our next set of experiments was performed in the backward mode with the optoacoustic probe. First, a turbid uniform gel slab (50 cm $\times$ 50 cm) with a thickness of 15 mm was made of gelatin (10%) and milk to simulate tissue with high scattering. The reduced scattering coefficient of the turbid gel, μ_s', was 2.9 cm^{-1}. The absorption coefficient of the turbid gel (μ_a = 0.11 cm^{-1}) was close to that of water (0.12 cm^{-1}) at the Nd:YAG laser wavelength of 1064 nm. These absorption and scattering coefficients yielded the effective attenuation coefficient μ_{eff} = 1.0 cm^{-1} typical of tissues with relatively low blood content in the near-IR spectral range.[6]

To simulate blood circulating in the SSS under the

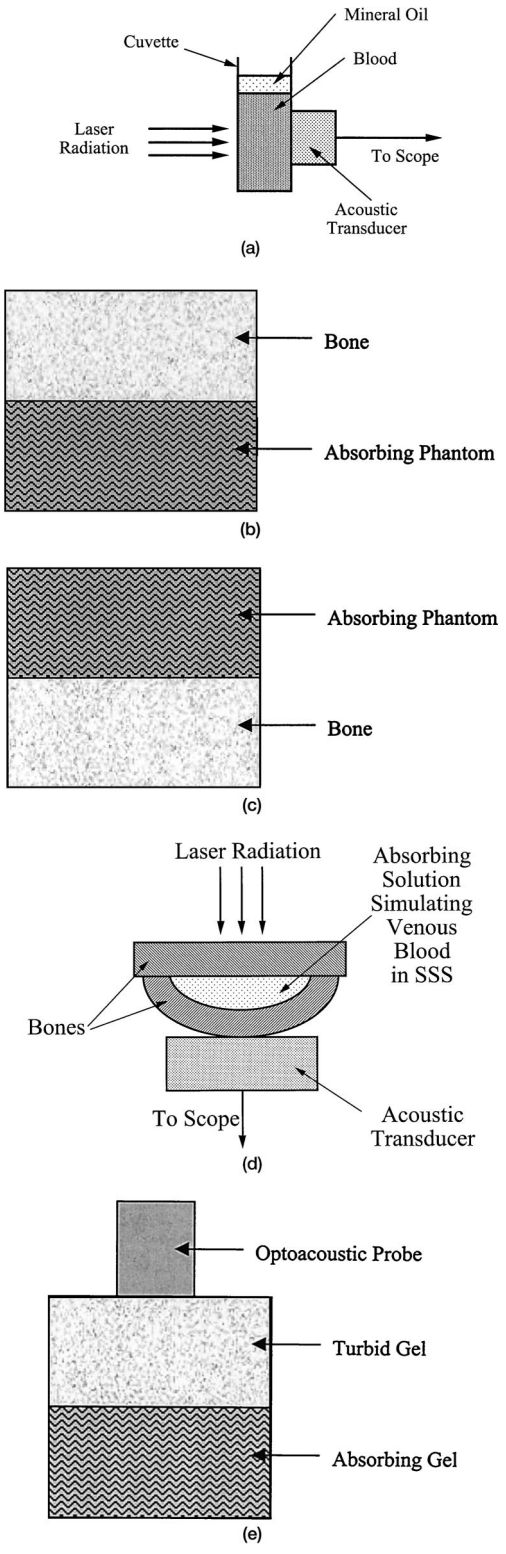

Fig. 2. (a) Irradiation of blood in a cuvette and detection by use of an acoustic transducer of optoacoustic waves induced in blood, (b) layered system with bone (on top) and an absorbing phantom used in the experiment on transmission of optical pulses through bone, (c) layered system with absorbing phantom (on top) and bone used in the experiment on acoustic transmission of optoacoustic waves through bone, (d) irradiation and detection of optoacoustic waves from an absorbing solution simulating venous blood through two bones, (e) layered system with turbid and absorbing gels used in the experiment with optoacoustic probe.

human skull, a layered tissue phantom was used [Fig. 2(e)]. The first 9.0-mm layer simulating the human skull was made of the same turbid gel. The second 9.0-mm layer was made of gel with a higher absorption coefficient (5 cm^{-1}) typical of venous blood in the near-IR spectral range. We achieved the higher absorption coefficient by adding Naphthol Green. The optoacoustic probe was placed on the surface of the uniform turbid phantom or the layered phantom, and data acquisition was performed.

We also evaluated the performance of our system *in vitro* with use of a blood-primed extracorporeal pump oxygenator (COBE Cardiovascular Inc., Arvada, Colo.), which circulated blood of varying oxygenation through a simulated SSS. The extracorporeal pump oxygenator consists of a reservoir in which blood accumulates, a supply of gases (oxygen, carbon dioxide, and nitrogen), a membrane oxygenator, an arterial tube (which, in patients, would be inserted into the aorta), a rotary pump, and a venous tube (which, in patients, would return blood from the great veins in the chest). In this model, the arterial and venous tubes were simply connected through a tissue phantom (that replicated features of tissue through which vessels course) to form a complete *ex vivo* circuit. By changing the gas supply into the membrane oxygenator and permitting time for equilibration, we can adjust the oxyhemoglobin saturation over a broad range, and we can also change the random order. For example, changing the gas supply to 95% oxygen results in nearly complete oxyhemoglobin saturation, whereas changing the gas supply to 5% oxygen results in oxyhemoglobin saturation of approximately 50%. Changing the gas supply below 5% provides oxyhemoglobin saturation below 50%.

To model the SSS, a thin-walled 5.0-mm tube was embedded in a plastic cuvette with 7.0-mm walls. The tube was connected to the oxygenator. Blood at different oxygenation was circulating through the tube. The signals were recorded in the backward mode through a 5.0-mm slab (made of the same turbid gel) and the cuvette. Blood samples (1.0 ml) were taken simultaneously with the optoacoustic data acquisition, and blood oxygenation was measured with the CO-Oximeter.

4. Results

Blood in the cuvette was irradiated by laser pulses as shown in Fig. 2(a). Ultrasonic gel was used to provide acoustic contact between the acoustic transducer and the cuvette. Optoacoustic pressure waves induced in the blood propagated to the transducer and were recorded on the scope. The optoacoustic pressure signals recorded at different blood oxygenation are displayed in Fig. 3(a). Variation of blood oxygenation dramatically changed the amplitude and slope of the pressure signals. The amplitude of the optoacoustic pressure, presented in Fig. 3(b) as a function of blood oxygenation, increased linearly as blood oxygenation increased. The amplitude of optoacoustic pressure recorded from pure arterial blood (92.6% saturation) was approximately 1.6 times

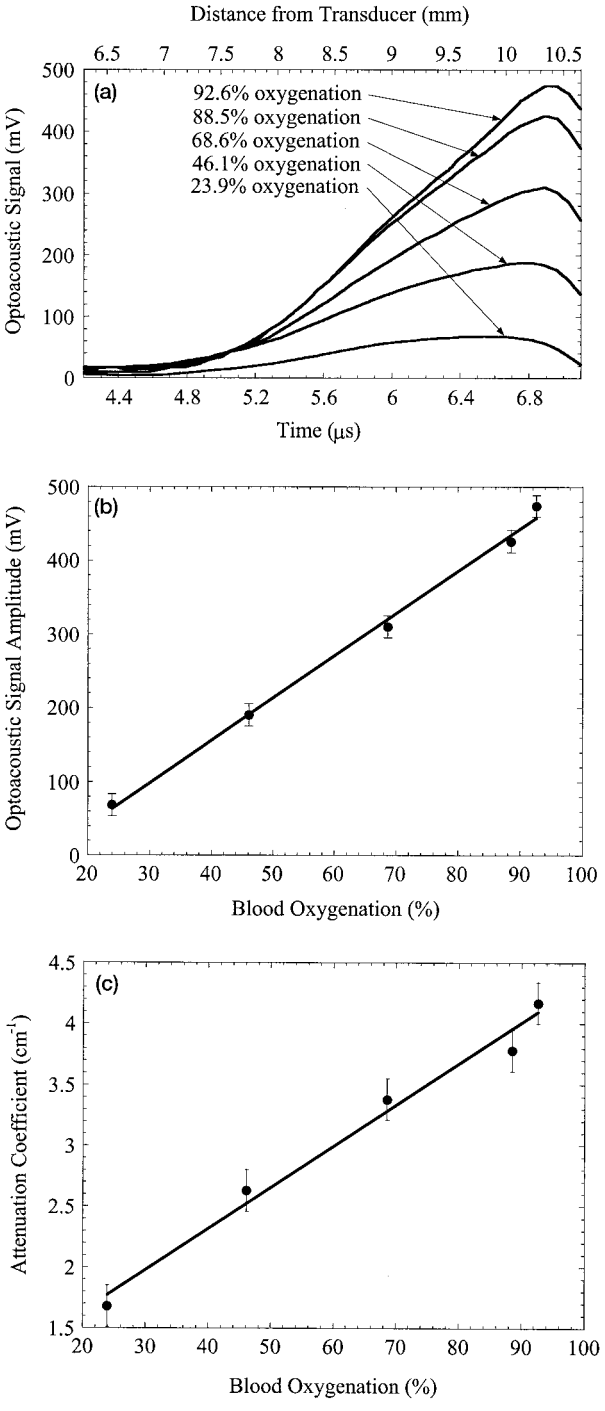

Fig. 3. (a) Optoacoustic signals measured from blood with different oxygenation, (b) optoacoustic signal amplitude as a function of blood oxygenation, (c) attenuation coefficient of blood calculated from the optoacoustic signals at different blood oxygenation.

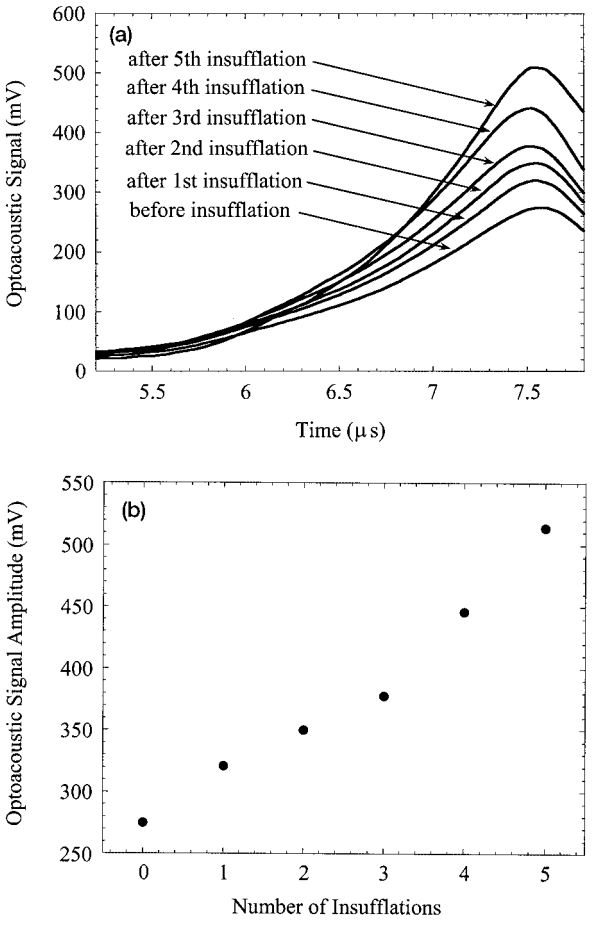

Fig. 4. (a) Optoacoustic signals detected from blood before and after insufflation of air, (b) amplitude of optoacoustic signal detected from blood before and after insufflation of air.

greater than that from normal venous blood (68.6% saturation). The amplitude in normal venous blood was approximately fourfold greater than in venous blood obtained during severe hemorrhagic shock (23.9% saturation).

In our experiment, the optoacoustic pressure slope was linearly dependent on blood oxygenation [Fig. 3(c)]. We calculated the slope of the optoacoustic signals by using the exponential fit of the signals. Because the speed of sound in blood is known (1.5 mm/μs), we calculated the blood attenuation coefficient at different oxygenation by converting the temporal scale into the spatial distribution of light in blood. The blood attenuation coefficient calculated from the optoacoustic pressure signals was approximately 4.2, 3.5, and 1.8 cm^{-1} for pure arterial, normal venous, and desaturated venous blood, respectively. This yields a 20% difference in the attenuation coefficient between arterial and normal venous blood and a 100% difference between normal and desaturated venous blood.

The optoacoustic signals were recorded after each insufflation [Fig. 4(a)]. One can see that each insufflation changes both the amplitude and the profile of the optoacoustic signals. Figure 4(b) shows that the optoacoustic signal amplitude increases from values typical of venous blood (275 mV) to that typical of arterial blood (510 mV). The delay between the optoacoustic data acquisitions (several seconds) was limited by the time required for insufflation.

Transmission of the Nd:YAG laser radiation with the wavelength of $\lambda = 1064$ nm through bone is presented in Fig. 5(a) as a function of bone thickness.

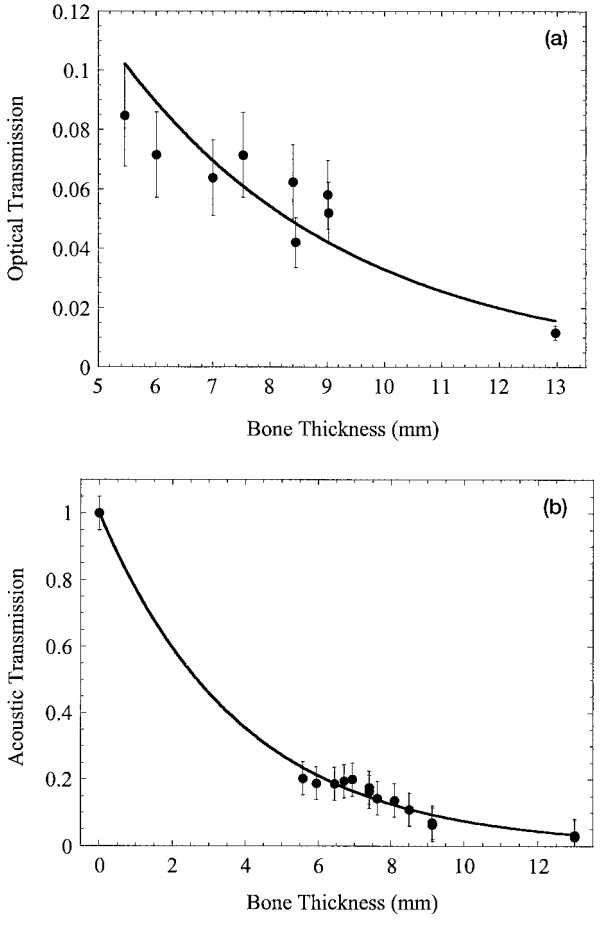

Fig. 5. (a) Optical transmission through bone samples of different thickness, (b) transmission of optoacoustic waves through bone samples of different thickness.

The curve represents an exponential fit to the experimental data points. These results show that approximately 3% of pulse energy is transmitted through bone of 10-mm thickness. The error in the data points is caused by variation in the optical properties of the bone samples. Experiments on transmission of optoacoustic pressure waves through bone [Fig. 5(b)] showed that the amplitude decreases by a factor of 12.5 at a bone thickness of 10 mm compared with the amplitude of the incident pressure wave. By using the phantom with two bones and an absorbing solution [Fig. 2(d)], we simulated simultaneously optical and acoustic attenuation of laser pulses and optoacoustic waves in bone tissue. A signal with an amplitude of approximately 200 mV was detected at a laser-pulse energy of 5.0 mJ and a laser fluence of 0.05 J/cm^2 (Fig. 6). The noise level of the registration system was 0.5 mV.

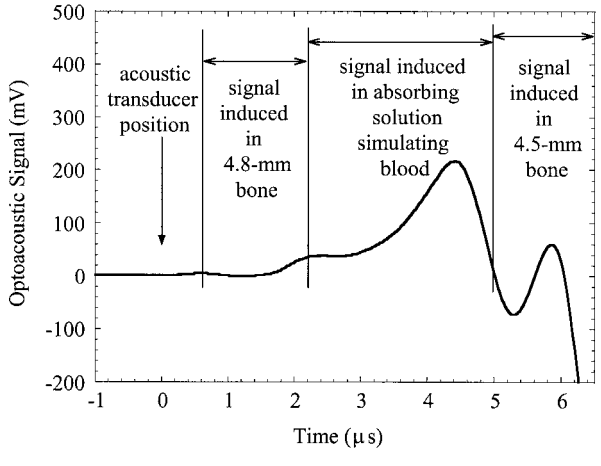

Fig. 6. Optoacoustic signal recorded from the absorbing solution simulating venous blood in the SSS.

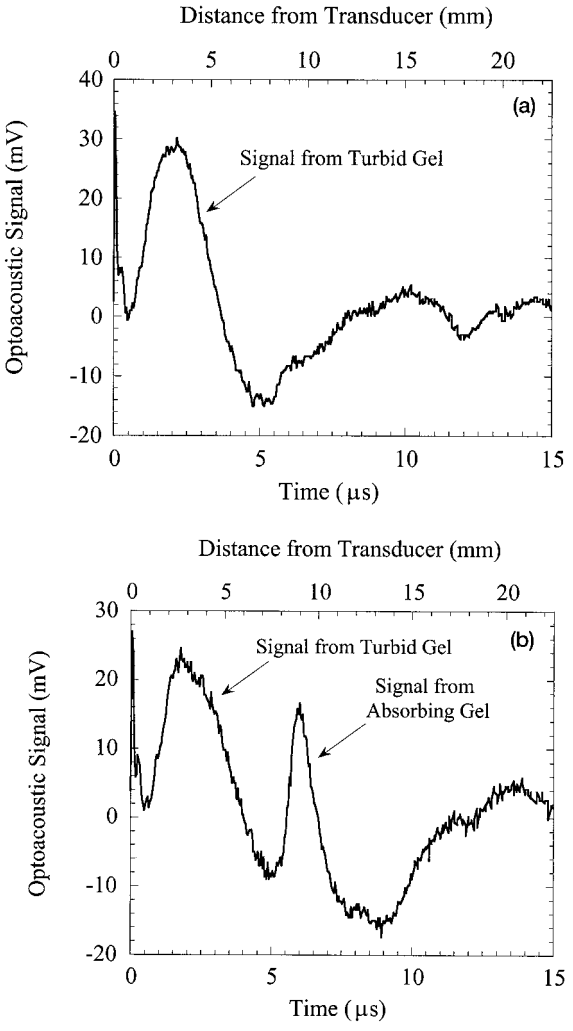

Fig. 7. (a) Optoacoustic signal recorded with the optoacoustic probe from 15-mm turbid uniform gelatin simulating thick tissue; (b) optoacoustic signal recorded with the optoacoustic probe from a layered tissue phantom (9-mm turbid gelatin slab and a slab of absorbing gelatin simulating blood under thick tissue).

Figure 7(a) shows an optoacoustic signal recorded in the backward mode by use of the optoacoustic probe from the 15-mm gel slab with the optical properties typical for tissues such as skull and skin in the near-IR spectral range. The first peak was due to optoacoustic wave generation on the surface of the probe by laser light reflected back from the scattering gel. The second (wide) peak with the following neg-

ative deflection was due to optoacoustic wave generation in the turbid gel. This optoacoustic signal is typical for uniform media. The signal recorded from the layered phantom [Fig. 7(b)] had one more peak at 5.95 μs. This peak was produced in the absorbing gel.

Optoacoustic signals were recorded with the optoacoustic probe in the backward mode from blood with different oxygenation circulating in the 5.0-mm latex tube simulating the SSS [Fig. 8(a)]. Oxyhemoglobin saturation was varied by the blood oxygenator. The measurements were performed through the turbid gel slab simulating tissue in the near-IR spectral range. The signals are presented in Fig. 8(b). The optoacoustic signals were recorded from the phantom at different levels of blood hemoglobin saturation (100, 90, 44, 27, and 10%). The first peak was produced by generation of optoacoustic waves directly on the surface of the optoacoustic probe. The long signal with the wide maximum at 2.4 μs was due to optoacoustic wave generation in the turbid gel. The signal between 5.0 and 8.0 μs was generated in blood circulating in the tube. The parameters of the signal clearly are dependent on blood oxygenation. The amplitude [Fig. 8(c)] and slope [Fig. 8(d)] of the signal increased linearly with blood oxygenation because of a higher absorption coefficient of oxyhemoglobin compared with that of deoxyhemoglobin. To calculate the slope of the optoacoustic signals measured in the backward mode, we normalized the signals induced in blood. The slope of the normalized signals is not dependent on amplitude and increases linearly with blood oxygenation. Therefore the measurement of the normalized signal slope can be used to monitor blood oxygenation in a vessel in the backward mode because the slope is not dependent on optical and acoustic transmission of tissues between the probe and the blood in the vessel.

5. Discussion

The amplitude and the slope of optoacoustic waves increase linearly with blood oxygenation [Figs. 3(a) and 3(b)] because of a higher absorption coefficient of oxyhemoglobin compared with that of deoxyhemoglobin at the Nd:YAG laser wavelength. Increasing hemoglobin saturation raises the hemoglobin absorption coefficient that then increases the blood attenuation coefficient [Fig. 3(c)], which was calculated from the optoacoustic signals by use of the exponential fit of the slope. The linear dependence of the optoacoustic amplitude and slope on blood oxygenation can be used for absolute measurement of blood oxygenation. The slope of the signal is more appropriate for continuous monitoring, because *in vivo* the amplitude of the optoacoustic waves recorded from blood will also depend on the thickness of tissues between blood and the optoacoustic probe, the variation of optical and acoustic transmission of these tissues, and the diffraction of optoacoustic waves that is due to propagation from blood to the probe. These parameters vary from patient to patient and may change in one patient during blood oxygenation mon-

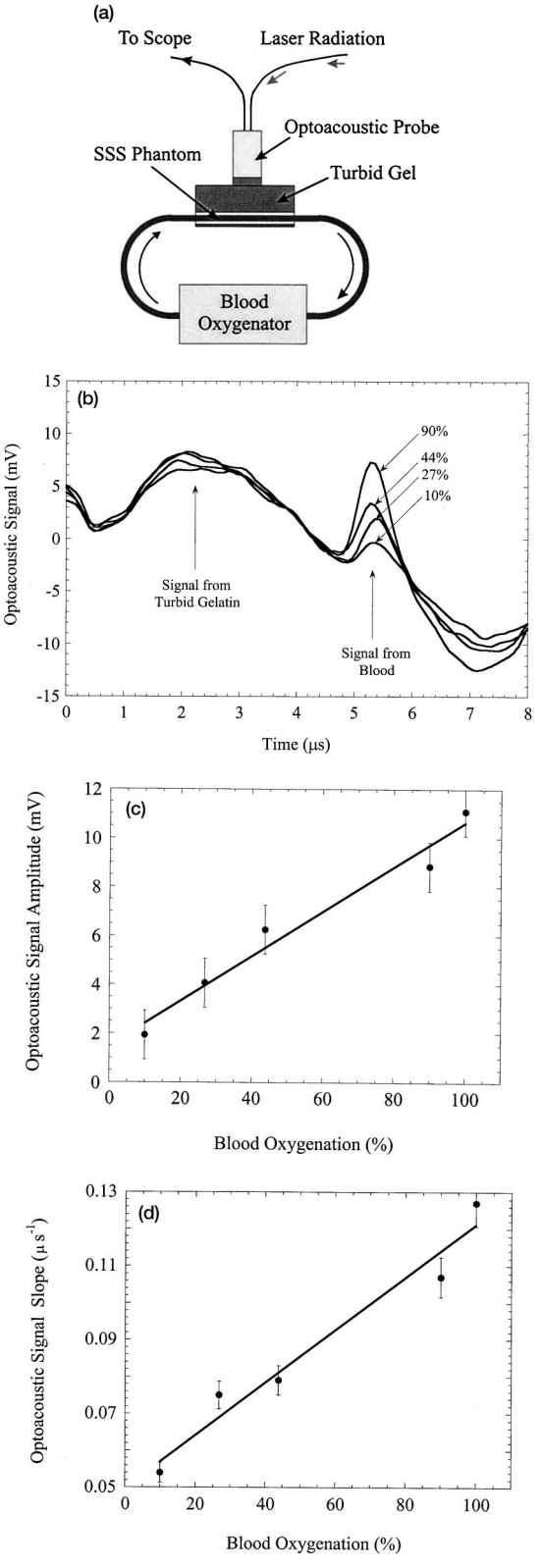

Fig. 8. (a) Measurement of optoacoustic signals through a turbid tissue phantom with the optoacoustic probe from blood with different oxygenation circulating in the SSS phantom, (b) optoacoustic signals recorded with the optoacoustic probe from the SSS phantom with blood at different oxyhemoglobin saturation (90, 44, 27, and 10% saturation) circulating in a 5-mm tube, (c) optoacoustic signal amplitude as a function of circulating blood oxygenation, (d) optoacoustic signal slope as a function of circulating blood oxygenation.

itoring. In contrast, the optoacoustic pressure slope is defined only by the optical properties of blood and is not influenced by variations in these parameters. The diffraction effect can be corrected by application of the algorithm reported in references 12 and 16. Therefore we anticipate that the optoacoustic pressure slope may provide quantitative measurements of blood oxygenation *in vivo*.

Rapid changes in blood oxygenation induced by incremental air insufflation with a syringe did not provide uniform oxygenation in the samples. This prevented accurate measurement of the optoacoustic pressure slope of the signals recorded immediately after each insufflation. However, *in vivo* blood oxygenation in large veins is uniformly mixed. Only use of the extracorporeal pump oxygenator provided homogeneity of blood and rates of changes in blood oxygenation that are typical of *in vivo* situations. Consequently, the experiments with the oxygenator are more representative of the expected performance in large animals and humans.

Each air insufflation took several seconds in our experiment. This limited the speed of data acquisition in the experiments on rapid changes in blood oxygenation. Optoacoustic data acquisition and processing with this system can be performed every second. A similar optoacoustic system has been used for real-time monitoring of rapid changes in tissue temperature as well as changes in optical properties during tissue hyperthermia and coagulation.[20,21] Therefore blood oxygenation can be measured every second with the optoacoustic technique. These results show that (1) blood oxygenation can be monitored continuously and (2) rapid changes (within seconds) in blood oxygenation can be detected with the optoacoustic technique.

Optoacoustic wave amplitude induced in tissue slightly increases (approximately 1.5%/°C) when tissue is heated in the range from 30 °C to 41 °C.[20,21] This is due to the increase of the tissue Grüneisen parameter with temperature.[20,21] The temperature-induced variation of optoacoustic signal amplitude cannot change the slope of the optoacoustic signals induced in blood because it is dependent only on optical properties of blood. Changes in blood optical properties can be produced only at higher temperatures (more than 50 °C) that are used for thermotherapy (thermal coagulation of tissue). However, these temperatures are not expected when thermotherapy is not used. Therefore thermally induced changes in optoacoustic wave parameters cannot decrease the accuracy of blood oxygenation measurement with this technique.

The data obtained in the experiment on optical and acoustic transmission through thick bone demonstrate that optoacoustic signals induced in blood circulating in the SSS can be measured with an acceptable signal-to-noise ratio. Moreover, we anticipate that both optical and acoustic transmission through bone *in vivo* will be greater than *in vitro*. Under *in vitro* conditions, dessication produces air pockets that decrease acoustic and optical transmission. The skin and dura are thin and have optical and acoustic transmission substantially better than the skull. Therefore we anticipate that overall optical and acoustic transmission *in vivo* through the tissues between the optoacoustic probe and the SSS will be sufficient for accurate measurement of blood oxygenation with high signal-to-noise ratio.

The optoacoustic probe, which combines optical fibers and a piezoelement, allowed measurement of optoacoustic waves in the backward mode. The experiments on layered gel and the SSS phantom demonstrated that optoacoustic signals were detected by the probe through thick scattering gels from absorbing layers [Figs. 7(a) and 7(b)] and blood circulating in the 5.0-mm tube simulating a blood vessel [Fig. 8(b)]. Both the amplitude and the slope of the signals recorded from blood increased linearly with blood oxygenation [Figs. 8(c) and 8(d)]. Therefore these experiments demonstrate the capability of the optoacoustic technique to detect changes in blood oxygenation continuously, noninvasively, and in real time through a tissuelike turbid medium with the optoacoustic probe. The signal-to-noise ratio can be substantially increased with further optimization of the parameters of the probe as well as the preamplifier.

Optoacoustic signal parameters are dependent not only on blood oxygenation but also on total hemoglobin concentration. This is because the blood absorption coefficient is dependent on total hemoglobin concentration. To provide accurate values of blood oxygenation despite variations of total hemoglobin concentration, one can use a measurement of optoacoustic waves induced at two different wavelengths. An Alexandrite laser with a wavelength of 750 nm can be used as a second source of pulsed laser radiation in the near-IR spectral range. Because oxygenated and deoxygenated hemoglobin have different absorption at the Nd:YAG and Alexandrite laser wavelengths, one can measure optoacoustic signals at these two wavelengths and calculate blood oxygenation by solving two equations:

$$\mu_a(1064) = C[\text{oxy}] \times K[\text{oxy}, 1064] + C[\text{deoxy}] \times K[\text{deoxy}, 1064], \quad (5)$$

$$\mu_a(750) = C[\text{oxy}] \times K[\text{oxy}, 750] + C[\text{deoxy}] \times K[\text{deoxy}, 750], \quad (6)$$

where μ_a (1064) and μ_a (750) are absorption coefficients of blood measured by the two-wavelength optoacoustic system at 1064 and 750 nm, respectively; C[oxy] and C[deoxy] are concentrations of oxyhemoglobin and deoxyhemoglobin in blood; and K [oxy, 1064], K [deoxy, 1064], K [oxy, 750], and K [deoxy, 750] are known values of extinction coefficients of oxyhemoglobin and deoxyhemoglobin at these two wavelengths. Having the two equations and the two unknowns (C[oxy] and C[deoxy]), one can calculate C[oxy] and C[deoxy] and hence oxygenation of the blood circulating in a vessel that is determined as the

ratio $C[\text{oxy}]/(C[\text{oxy}] + C[\text{deoxy}])$. Therefore use of the two-wavelength approach can provide absolute values of blood oxygenation with high accuracy at different hemoglobin concentrations. We believe that the two-wavelength system can accurately measure cerebral blood oxygenation at a variation of other physiological parameters of the patient (temperature, intracranial pressure, blood flow) because they can produce only minor changes in the parameters of the optoacoustic wave recorded from the SSS.

Because Nd:YAG and Alexandrite can produce short (nanosecond) optical pulses with sufficient energy and are commercially available, they are good candidates for the two-wavelength system. However, any other lasers that can produce short pulses in the near-IR spectral range can be used for the two-wavelength optoacoustic system including pulsed laser diodes. Use of the pulsed laser diodes in optoacoustic systems can dramatically decrease dimensions, weight, and cost of the systems because they are substantially smaller, lighter, and less expensive than the solid-state lasers. Recent progress in the development of laser diodes with nanosecond pulse duration and high pulsed power indicates that the laser diodes can potentially be used in optoacoustic systems, including the systems for cerebral blood oxygenation monitoring. Currently, we are developing a laser diode optoacoustic system that will have less weight, dimensions, and cost compared with the systems based on the solid-state lasers.

6. Conclusion

We developed, built, and tested *in vitro* a laser optoacoustic system with a probe designed for noninvasive monitoring of blood oxygenation in structures such as the SSS. Our results demonstrated that (1) the amplitude and temporal profile of the optoacoustic waves are linearly dependent on blood oxygenation in the wide range of blood oxygenation from 24% to 92%; (2) the system is capable of real-time and continuous measurements; (3) optoacoustic signals can be detected despite optical and acoustic attenuation by thick bone; and (4) the system is capable of blood oxygenation measurements in model 5.0-mm veins through thick, light-scattering tissue phantoms. We believe that the optoacoustic technique can potentially be used for noninvasive, accurate, and continuous monitoring of blood oxygenation in both cerebral and systemic veins. Our next investigation will focus on *in vivo* tests of the system in large animals. Our specific plan is to monitor cerebral blood oxygenation in the sheep SSS.

These studies are supported in part by grant 1 R21 NS40531-01 from the National Institutes of Health.

References

1. D. S. Prough, V. Yancy, and D. J. Deyo, "Brain monitoring: considerations in patients with craniocerebral missile wounds," in *Missile Wounds of the Head and Neck*, B. Aarabi and H. H. Kaufman, eds., (The American Association of Neurosurgical Surgeons, Rolling Meadows, Ill., 1999), pp. 221–253.
2. A. Zauner, E. M. Doppenberg, J. J. Woodward, S. C. Choi, H. F. Young, and R. Bullock, "Continuous monitoring of cerebral substrate delivery and clearance: initial experience in 24 patients with severe acute brain injuries," Neurosurgery **41,** 1082–1093 (1997).
3. V. Pollard, D. S. Prough, A. E. DeMelo, D. J. Deyo, T. Uchida, and H. F. Stoddart, "Validation in volunteers of a near-infrared spectroscope for monitoring brain oxygenation in vivo," Anesth. Analg. **82,** 269–277 (1996).
4. V. Pollard, D. S. Prough, A. E. DeMelo, D. J. Deyo, T. Uchida, and R. Widman, "The influence of carbon dioxide and body position on near-infrared spectroscopic assessment of cerebral hemoglobin oxygen saturation," Anesth. Analg. **82,** 278–287 (1996).
5. S. Wray, M. Cope, D. T. Deply, J. S. Wyatt, and E. O. R. Reynolds, "Characterization of the near infrared absorption spectra of cytochrome aa_3 and hemoglobin for the non-invasive monitoring of cerebral oxygenation," Biochim. Biophys. Acta **933,** 184–192 (1988).
6. A. J. Welch and M. J. C. Van Gemert, *Optical-Thermal Response of Laser-Irradiated Tissue* (Plenum, New York, 1981).
7. V. Pollard and D. S. Prough, "Cerebral oxygenation: near-infrared spectroscopy," in *Principles and Practice of Intensive Care Monitoring*, M. J. Tobin, ed., (McGraw-Hill, New York, 1988), pp. 1019–1033.
8. B. Chance, J. S. Leigh, H. Miyake, D. S. Smith, S. Nioka, R. Greenfeld, M. Finander, K. Kaufmann, W. Levy, M. Young, P. Cohen, H. Yoshioka, and R. Boretsky, "Comparison of time-resolved and -unresolved measurements of deoxyhemoglobin in brain," Proc. Natl. Acad. Sci. USA **85,** 4971–4975 (1988).
9. M. F. Newman, E. Lowry, N. D. Croughwell, W. White, J. Kirchner, J. Blumenthal, and The Neurologic Outcome Research Group, "Near-infrared spectroscopy (INVOS 3100 A) and cognitive outcome after cardiac surgery," Anesth. Analg. **84**(**2S**)**,** S111 (1997).
10. M. S. Patterson, B. Chance, and B. C. Wilson, "Time resolved reflectance and transmittance for the noninvasive measurement of tissue optical properties," Appl. Opt. **28,** 2331–2336 (1989).
11. R. O. Esenaliev, K. V. Larin, I. V. Larina, M. Motamedi, and D. S. Prough, "Optoacoustic technique for non-invasive continuous monitoring of blood oxygenation," in *Biomedical Topical Meetings*, Postconference Digest, Vol. 38 of OSA Trends in Optics and Photonics (Optical Society of America, Washington, D.C., 2000), pp. 272–274.
12. V. E. Gusev and A. A. Karabutov, *Laser Optoacoustics* (American Institute of Physics, New York, 1993).
13. R. O. Esenaliev, A. A. Oraevsky, V. S. Letokhov, A. A. Karabutov, and T. V. Malinsky, "Studies of acoustical and shock waves in the pulsed laser ablation of biotissue," Lasers Surg. Med. **13,** 470–484 (1993).
14. A. A. Oraevsky, S. L. Jacques, R. O. Esenaliev, and F. K. Tittel, "Laser-based optoacoustic imaging in biological tissues," in *Laser-Tissue Interaction V*, S. L. Jacques, ed., Proc. SPIE **2134A**, 122–128 (1994).
15. A. A. Oraevsky, R. O. Esenaliev, S. L. Jacques, and F. K. Tittel, "Laser optoacoustic tomography for breast cancer diagnostics," in *Advances in Optical Imaging and Photon Migration*, R. R. Alfano and J. G. Fujimoto, eds., Vol. 2 of OSA Trends in Optics and Photonics Series (Washington, D.C., Optical Society of America, 1996), pp. 316–321.
16. R. O. Esenaliev, H. Alma, F. K. Tittel, and A. A. Oraevsky, "Axial resolution of laser opto-acoustic imaging: influence of acoustic attenuation and diffraction," in *Laser-Tissue Interaction IX*, S. L. Jacques, ed., Proc. SPIE **3254,** 294–301 (1998).
17. R. O. Esenaliev, A. A. Karabutov, and A. A. Oraevsky, "Sensitivity of laser opto-acoustic imaging in detection of small

deeply embedded tumors," IEEE J. Sel. Top. Quantum Electron. **5,** 981–988 (1999).
18. S. P. Gopinath, C. S. Robertson, C. F. Contant, C. Hayes, Z. Feldman, R. K. Narayan, and R. G. Grossman, "Jugular venous desaturation and outcome after head injury," J. Neurol. Neurosurg. Psychiatry **57,** 717–723 (1994).
19. N. D. Croughwell, M. F. Newman, J. A. Blumenthal, W. D. White, J. B. Lewis, P. E. Frasco, L. R. Smith, E. A. Thyrum, B. J. Hurwitz, B. J. Leone, R. M. Schell, and J. G. Reves, "Jugular bulb saturation and cognitive dysfunction after cardiopulmonary bypass," Ann. Thorac. Surg. **58,** 1702–1708 (1994).
20. R. O. Esenaliev, I. V. Larina, K. V. Larin, and M. Motamedi, "Real-time optoacoustic monitoring during thermotherapy," in *Biomedical Optoacoustics*, A. O. Oraevsky, ed., Proc. SPIE **3916,** 302–310 (2000).
21. K. V. Larin, I. V. Larina, M. Motamedi, and R. O. Esenaliev, "Monitoring of temperature distribution with optoacoustic technique in real time," in *Biomedical Optoacoustics*, A. O. Oraevsky, ed., Proc. SPIE **3916,** 311–321 (2000).